

Coulomb energy and correlations of inversion-layer electrons in metal-oxide-semiconductor field-effect transistor devices

A. Widom and R. Tao

Department of Physics, Northeastern University, Boston, Massachusetts 02115

(Received 11 March 1988; revised manuscript received 30 June 1988)

The effective Coulomb potential between inversion layer electrons in metal-oxide-semiconductor field-effect transistor devices is computed, including the screening due to induced charges on the metal plate of the gate capacitor. Significant deviations from the usual Coulomb energy appear when the electron spacing is equal to or larger than the distance between the inversion layer and the metal plate. The energy of a Wigner crystal in this model is calculated. The hexagonal lattice has a lower energy than the square lattice. The upper bound of the free energy associated with the screened potential in a magnetic field is estimated.

I. INTRODUCTION

Silicon metal-oxide-semiconductor field-effect devices¹ (MOSFETs) and GaAs-Ga_xAl_{1-x}As heterojunctions² are important devices in fundamental research and technology. Since the discovery of the quantum Hall effect on these devices,^{3,4} their importance in fundamental research has been greatly enhanced.

In the theoretical research on the two-dimensional electron system, the jellium model has been conventionally employed, which has electrons moving in a positive neutralizing uniform background.⁵ As noticed by Lenard and Dyson⁶ and Lieb and Narnhofer⁷ the jellium model usually has some fundamental problems. For example, classical jellium does not have thermodynamic stability; it violates the convexity condition normally associated with the second law of thermodynamics.

In reality, the two-dimensional electrons in the inversion layer of a MOSFET device are a finite distance away from the positive metal plate,¹ which makes the devices, in some sense, similar to a microcapacitor. The two-dimensional electron gas at GaAs-Ga_xAl_{1-x}As interface is also separated from the positive charged donors by a small distance.^{2,8} As it will be shown later, this finite distance separation makes a significant difference between the jellium model and the real two-dimensional devices. The present paper is devoted to study of the Coulomb energy and correlations of two-dimensional electrons in the real physical devices. While the discussion will be mainly about MOSFET devices, it is noted that the results may also be true for GaAs-Ga_xAl_{1-x}As heterojunctions. In previous studies, similar models were employed to consider the effect on mobility⁹ and discuss electrons on films of liquid helium.¹⁰

In typical MOSFET devices, the electron density n is of order $2 \times 10^{11} \text{ cm}^{-2}$ and the distance between the inversion layer and the gate metal plate L is of the order of 100 Å. In GaAs-Ga_xAl_{1-x}As heterojunctions n is about 10^{12} cm^{-2} and L is about several hundred angstroms. From the above data, the mean spacing between electrons is also of the order of 100 Å. We introduce a dimensionless quantity

$$\alpha = 1/L\sqrt{n} \quad , \quad (1.1)$$

which is the ratio of the mean spacing between electrons and the distance between two capacitor plates. In classical capacitors, α is vanishingly small; then the Coulomb energy is usually written as

$$U_0 = (Ne)^2 / 2C_g \quad , \quad (1.2)$$

where C_g is the geometrical capacitance

$$C_g = \epsilon A / 4\pi L \quad . \quad (1.3)$$

A is the area of the plates and ϵ is the dielectric constant. Thus, in the simple capacitor view, the Coulomb energy per unit area is given by

$$U_0 / A = (2\pi e^2 / \epsilon) Ln^2 \quad , \quad (1.4)$$

where $n = N/A$. In MOSFET devices, α may be of the order of unity or even larger. Then many electron correlations must appear in the Coulomb energy.

In what follows, it will be argued that the effective electrostatic potential between two electrons with distance R on the inversion layer has the form

$$v(R) = (e^2 / \epsilon R) \chi(R/L) \quad , \quad (1.5)$$

where $\chi(x)$ is a screening function due to induced charges on the metal plate of the gate capacitor. In the model to be discussed $\chi(x)$ is a non-negative function obeying the sum rule

$$\int_0^\infty \chi(x) dx = 2 \quad . \quad (1.6)$$

Thus, if $g(r)$ denotes the radial distribution of electrons in the inversion layer as seen by a given electron, then the usual expression for the mean (two-body) potential energy of an interacting system in two dimensions

$$U/A = \pi n^2 \int_0^\infty dr rv(r)g(r) \quad . \quad (1.7)$$

A useful form of Eq. (1.7) follows from Eq. (1.5),

$$U/A = (\pi e^2 / \epsilon) n^2 L \int_0^\infty dx \chi(x)g(xL) \quad , \quad (1.8)$$

i.e., the simple capacitor Coulomb energy Eq. (1.4) is a consequence of the sum rule of Eq. (1.6), if the radial distribution in Eq. (1.8) is approximated by $g(xL) = g(x/\alpha\sqrt{n}) \approx 1$. This approximation is adequate only if α is vanishingly small. However, this condition does not hold true for most MOSFET devices. Thus, many-electron correlation must appear in the Coulomb energy. In Sec. II, the electrostatic Green's function will be discussed, and the screening function $\chi(R/L)$ will be derived. In Sec. III, the static ground-state energy of a two-dimensional Wigner crystal has been calculated for square lattice and hexagonal lattice. At a constant electron density, the hexagonal lattice has the lower energy. In Sec. IV, estimation of the free energy of the model in the magnetic field will be discussed. In the concluding Sec. V, the adequacy of using purely electrostatic potentials will be put at issue. The point is that electronic two-body interactions arise from one-photon exchange. The importance of fully quantum electrodynamic photon propagator (with the metal renormalization¹¹) will be stressed.

II. ELECTROSTATICS

Let the metal plate of the gate capacitor be the plane $z=0$ so that the plane of the inversion layer is at $z=L$. The potential at the metal plate is V_0 , a positive constant. Between these two planes, the electrostatic potential

$$\phi(x, y, z) + V_0 = \phi(\mathbf{R}, z) + V_0 \quad (2.1)$$

obeys the Laplace equation

$$\Delta\phi = [\Delta_{\mathbf{R}} + (\partial/\partial z)^2]\phi = 0, \quad (2.2)$$

where the two-dimensional vector $\mathbf{R}=(x, y)$. From Eq. (2.1) at the metal plate $z=0$,

$$\phi(\mathbf{R}, 0) = 0, \quad (2.3)$$

The effective charge per unit area $\sigma(\mathbf{R})$ at the inversion layer will be defined by the boundary condition

$$\epsilon \frac{\partial\phi(\mathbf{R}, z=L)}{\partial z} = 4\pi\sigma(\mathbf{R}). \quad (2.4)$$

The gate capacitor electrostatic problem consists of the computation of the Green's function

$$\phi(\mathbf{R}, L) = \int G(\mathbf{R}-\mathbf{R}')\sigma(\mathbf{R}')d^2\mathbf{R}'. \quad (2.5)$$

Solving Eq. (2.2) via the Fourier decomposition

$$\phi(\mathbf{R}, z) = \int \frac{d^2\mathbf{k}}{(2\pi)^2} \phi_{\mathbf{k}}(z) e^{i\mathbf{k}\cdot\mathbf{R}} \quad (2.6)$$

yields, for $0 < z < L$,

$$[(\partial/\partial z)^2 - k^2]\phi_{\mathbf{k}}(z) = 0, \quad (2.7)$$

while the boundary condition Eqs. (2.3) and (2.4) read

$$\phi_{\mathbf{k}}(0) = 0, \quad (2.8a)$$

$$\epsilon \phi'_{\mathbf{k}}(L) = 4\pi \int d^2\mathbf{R} e^{-i\mathbf{k}\cdot\mathbf{R}} \sigma(\mathbf{R}). \quad (2.8b)$$

The solution to Eqs. (2.7) and (2.8) is

$$\phi_{\mathbf{k}}(z) = (4\pi/\epsilon k) [\sinh(kz)/\cosh(kL)] \sigma_{\mathbf{k}}, \quad (2.9)$$

where

$$\sigma_{\mathbf{k}} = \int d^2\mathbf{R} e^{-i\mathbf{k}\cdot\mathbf{R}} \sigma(\mathbf{R}). \quad (2.10)$$

Equations (2.5), (2.6), (2.9), and (2.10) yield the required Green's function

$$G(\mathbf{R}) = \left[\frac{4\pi}{\epsilon} \right] \int \frac{d^2k}{(2\pi)^2} \left[\frac{\tanh(kL)}{k} \right] e^{i\mathbf{k}\cdot\mathbf{R}}. \quad (2.11)$$

Performing the angular integration in Eq. (2.11) yields

$$G(\mathbf{R}) = \left[\frac{2}{\epsilon} \right] \int_0^\infty dk J_0(kR) \tanh(kL), \quad (2.12)$$

where $J_0(\eta)$ is the zero-order Bessel function. Writing Eq. (2.12) as a "screened" Coulomb Green's function

$$G(\mathbf{R}) = (1/\epsilon R) \chi(R/L) \quad (2.13)$$

yields the required screening function introduced in Sec. I, i.e.,

$$\begin{aligned} \chi(x) &= 2 \int_0^\infty J_0(\eta) \tanh(\eta/x) d\eta \\ &= 2 \sum_{n=-\infty}^{\infty} \frac{(-1)^n x}{(4n^2 + x^2)^{1/2}}. \end{aligned} \quad (2.14)$$

With the Poisson summation technique, Eq. (2.14) can be transformed into

$$\chi(x) = 4x \sum_{l=1}^{\infty} K_0(\frac{1}{2}\pi(2l-1)x), \quad (2.15)$$

where $K_0(x)$ is the modified Bessel function. Note that the sum rule Eq. (1.6) follows from Eqs. (2.14) and (2.15). Equation (2.15) is extremely convenient in numerical calculations since it converges very fast. In Fig. 1, the

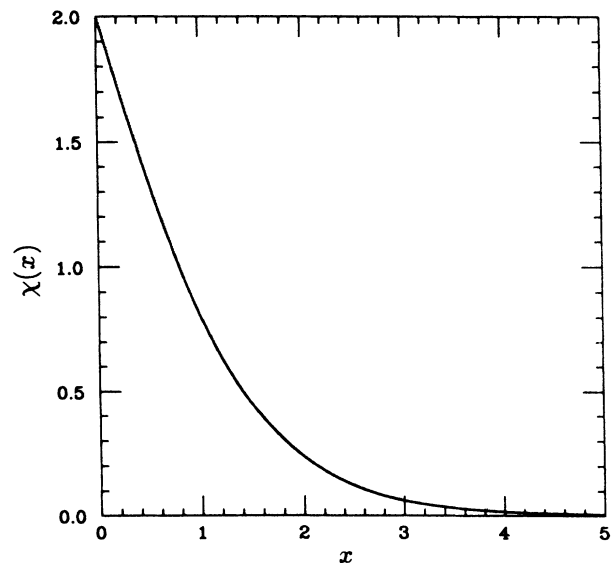


FIG. 1. The screening function $\chi(x)$, where x is the ratio of the distance between two electrons to the distance between the inversion layer and the metal plate.

screening function $\chi(x)$ is plotted. The effect of the induced charge density on the metal plate increases the short-ranged Coulomb repulsion between electrons in the inversion layer and decreases the long-ranged interaction. For example, when $x = R/L$ is close to 1, $\chi(x)$ is reduced to about 0.4 of $\chi(0)$. The length scale of the long-ranged screening is determined by the spacing L .

III. WIGNER LATTICE WITH SCREENING COULOMB INTERACTION

Now we consider the crystal state of our model. From Eqs. (2.13) and (2.14), the Coulomb energy with the screening interaction is given by

$$U_C = \frac{Ne^2}{2\epsilon} \sum_{j \neq 0} \chi(R_j/L)/R_j, \quad (3.1)$$

where $\mathbf{R}_j = j_1 \mathbf{a} + j_2 \mathbf{b}$, j_1 and j_2 are integers, \mathbf{a} and \mathbf{b} are primitive translation vectors of the lattice. In the square lattice, $\mathbf{a} = a\hat{x}$, $\mathbf{b} = a\hat{y}$, and in the hexagonal lattice, $\mathbf{a} = a\hat{x}$ and $\mathbf{b} = a[\frac{1}{2}\hat{x} + (\sqrt{3}/2)\hat{y}]$, where \hat{x} and \hat{y} are the unit vectors along the x direction and y direction, respectively, and a is the distance between the two nearest electrons in the lattice, given by

$$a = \begin{cases} 1/\sqrt{n} & \text{for a square lattice} \\ \left[\frac{2}{\sqrt{3n}} \right]^{1/2} & \text{for a hexagonal lattice.} \end{cases} \quad (3.2)$$

With $R_j = ar_j$, Eq. (3.1) reads

$$U_C = \frac{Ne^2}{2\epsilon L} \sum_{j \neq 0} \chi(r_j a/L)/(r_j a/L), \quad (3.3)$$

where $r_j = (j_1^2 + j_2^2)^{1/2}$ in the square lattice, and $r_j = (j_1^2 + j_1 j_2 + j_2^2)^{1/2}$ in the hexagonal lattice.

With Eq. (2.15), the static energies of both the square lattice and the hexagonal lattice have been calculated and are plotted in Fig. 2 as a function of $\alpha = 1/(L\sqrt{n})$, the ratio of the electron spacing to the spacing between two plates. The energy of the classical capacitor, $U_0 = 2\pi Ne^2 nL/\epsilon$, is taken as the energy unit in Fig. 2. It is clear from the figure that in the limit of $\alpha \rightarrow 0$, U_C tends to the classical energy U_0 . But as α increases, the energy reduces quickly. For example, as $\alpha = 1$, i.e., the electron spacing is comparable with the spacing between two plates, U_C is only about $0.4U_0$.

In Fig. 3, the Coulomb energy is plotted against A/NL^2 . The energy unit in Fig. 3 is $Ne^2/\epsilon L$. It is clear from the figure that the pressure is positive,

$$P = - \left(\frac{\partial U_C}{\partial A} \right)_{N,L}, \quad (3.4)$$

and the compressibility is also positive

$$\left(\frac{\partial P}{\partial n} \right)_{N,L} = - \frac{A^2}{N} \left(\frac{\partial^2 U_C}{\partial A^2} \right)_{N,L} > 0. \quad (3.5)$$

Therefore, the convexity condition of the model is satisfied.

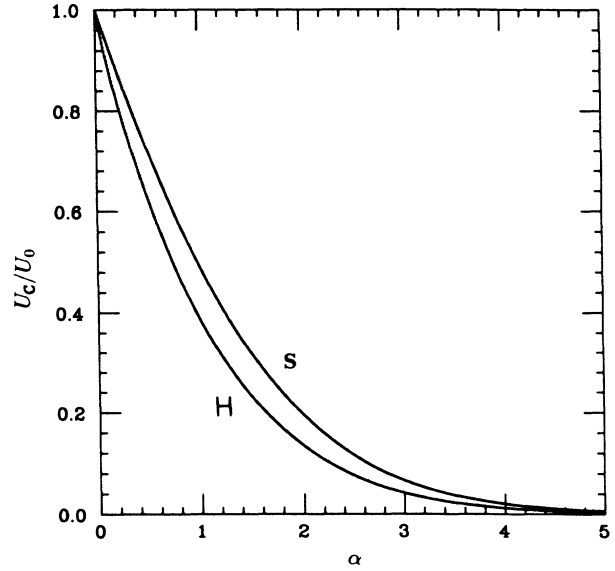


FIG. 2. The Coulomb energy U_C of the Wigner crystal vs $\alpha = 1/L\sqrt{n}$. The label "S" means the square lattice and the label "H" means the hexagonal lattice. $U_0 = 2\pi Ne^2 nL/\epsilon$ is the energy of the classical capacitor. Here n is the electron density, L is the distance between the inversion layer and the metal plate, ϵ is the dielectric constant, and N is the number of electrons.

From Figs. 2 and 3, at the same electron density, the hexagonal lattice always has a lower energy than the square lattice. This result was also found in the calculation of Wigner crystal for two-dimensional jellium.¹²

It is noted that if the electrons were uncorrelated and the charges were spread uniformly in the inversion layer,

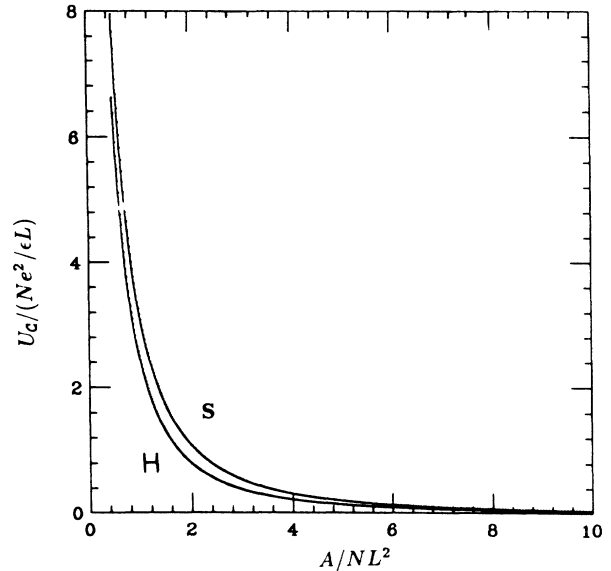


FIG. 3. The Coulomb energy U_C of the Wigner crystal vs $A/NL^2 = 1/L^2 n$. The label "S" means the square lattice. The label "H" means the hexagonal lattice. The energy unit is $Ne^2/\epsilon L$. Here N is the number of electrons, A is the area, $n = N/A$, and L is the distance between the inversion layer and the metal plate.

the Coulomb energy would equal to the classical energy U_0 . Our above results show that the Coulomb energy of the capacitor with uniform charge density is higher than the Coulomb energy of a correlated Wigner lattice.

IV. ESTIMATION OF THE FREE ENERGY IN A MAGNETIC FIELD

The effect of a magnetic field on the model is a topic presently under investigation. In this section, we will only estimate the upper bound for the free energy of the system in the presence of magnetic field. The Hamiltonian in this case is given by

$$H = H_0 + (e^2/\epsilon) \sum_{1 \leq i < j}^N (1/r_{ij}) \chi(r_{ij}/L), \quad (4.1)$$

where

$$H_0 = \frac{1}{2m} \sum_{j=1}^N \pi_j^2, \quad (4.2)$$

$$\pi_j = -i\hbar \partial / \partial \mathbf{r}_j - (e/c) \mathbf{A}(\mathbf{r}_j). \quad (4.3)$$

Since the potential energy is bounded from below by the crystal energy, the canonical partition function is bounded from above,

$$\Omega(N, B, T) = \text{Tr}(e^{-\beta H}) < e^{-\beta U_c} \Omega_0, \quad (4.4)$$

where $\beta = 1/k_B T$, $\Omega_0 = \text{Tr}(e^{-\beta H_0})$ is the canonical partition function of a two-dimensional free-electron gas in a magnetic field, and U_c is the potential energy of hexagonal Wigner lattice in Eq. (3.3). The grand canonical partition function is hence also bounded from above,

$$\Pi = \sum_{N=0}^{\infty} e^{-\beta N \mu} \Omega(N, T, B) < e^{-\beta U_c} \Pi_0, \quad (4.5)$$

where $\Pi_0 = \sum_{N=0}^{\infty} e^{-\beta N \mu} \Omega_0(N, T, B)$ is the grand canonical

partition function of the two-dimensional free electrons in the magnetic field. Since Π_0 is convergent, Π is also convergent. Then the grand canonical pressure exists and is estimated

$$P = k_B T \ln(\Pi) / A < k_B T \ln(\Pi_0) / A - U_c / A. \quad (4.6)$$

The convexity condition holds true. The jellium model under a strong magnetic field, on the other hand, violates the convexity condition.¹³

IV. DISCUSSION

For nonrelativistic two-dimensional interacting electrons in the inversion layers, we have proposed a two-electron potential

$$v(\mathbf{R}) = \frac{2e^2}{\epsilon R} \int_0^\infty J_0(\eta) \tanh(\eta L/R) d\eta, \quad (5.1)$$

which is more realistic and physical than the jellium model.

The effective charge density per unit area is defined (in the Coulomb Green's-function problem) via the normal component of the electric field, i.e., Eq. (2.4). An open problem concerns the tangential components of the electric field. In particular this requires consideration of transverse electromagnetic fields. Electrostatics is not the complete description of effective potentials. If the effective potential between electrons is computed, using quantum electrodynamic one-photon exchange, then the Green's-function calculation must be extended to include the full photon propagator $D_{\mu\nu}(x, y)$ via the action¹¹

$$W = \frac{1}{2c^3} \int d^4x \int d^4y J^\mu(x) D_{\mu\nu}(x, y) J^\nu(y). \quad (5.2)$$

The present paper also has neglected the thickness of inversion layers which will certainly produce a correction to the above results for "two-dimensional" inversion layers. The effects of transverse electromagnetic fields on long-range screening and the effect of finite thickness of inversion layers are presently under consideration.

¹T. Ando, A. B. Fowler, and F. Stern, *Rev. Mod. Phys.* **54**, 37 (1982).

²H. L. Störmer, R. Dingle, A. C. Gossard, W. Wiegmann, and M. D. Sturge, *Solid State Commun.* **29**, 705 (1979).

³K. von Klitzing, G. Dorda, and M. Pepper, *Phys. Rev. Lett.* **45**, 494 (1980).

⁴D. C. Tsui, H. L. Störmer, and A. C. Gossard, *Phys. Rev. Lett.* **48**, 1559 (1982).

⁵For example, see R. B. Laughlin, *Phys. Rev. Lett.* **50**, 1395 (1983); F. D. M. Haldane, *ibid.* **51**, 605 (1983); D. Yoshioka, B. I. Halperin, and P. A. Lee, *ibid.* **50**, 1219 (1983).

⁶A. Lenard and F. J. Dyson, *J. Math. Phys.* **9**, 698 (1968).

⁷E. L. Lieb and H. Narnhofer, *J. Stat. Phys.* **12**, 291 (1975), and references therein (their proof can be easily extended to the case with magnetic field); **14**, 465 (1976).

⁸G. A. Baraff and D. C. Tsui, *Phys. Rev. B* **28**, 1142 (1983).

⁹A. Gold, *Appl. Phys. Lett.* **48**, 439 (1986).

¹⁰U. de Freitas *et al.*, *J. Phys. C* **20**, 5983 (1987).

¹¹E. M. Lifshitz, and L. P. Pitaevskii, *Statistical Physics, Part 2* (Pergamon, Oxford, 1980), pp. 314–359.

¹²L. Bonsall and A. A. Mārādudin, *Phys. Rev. B* **15**, 1959 (1977).

¹³R. Tao, A. Widom, Z. C. Tao, and H. K. Sim, *Int. J. Mod. Phys. B* (to be published).